Journal of Photochemistry & Photobiology, B: Biology 252 (2024) 112860

Contents lists available at ScienceDirect

Journal of Photochemistry & Photobiology, B: Biology

journal homepage: www.elsevier.com/locate/jphotobiol

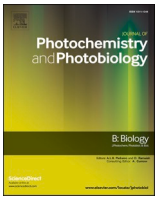

Effects of antimicrobial photodynamic therapy with photodithazine® on methicillin-resistant *Staphylococcus aureus* (MRSA): Studies in biofilms and experimental model with *Galleria mellonella*

Beatriz Müller N. Souza [a], Alejandro Guillermo Miñán [b], Isabelle Ribeiro Brambilla [a], Juliana Guerra Pinto [a,*], Maíra Terra Garcia [c], Juliana Campos Junqueira [c], Juliana Ferreira-Strixino, PhD [a,*]

[a] *Photobiology Applied to Health (PhotoBioS Lab), Universidade do Vale do Paraíba (UNIVAP), São José dos Campos, São Paulo, Brazil*
[b] *Instituto de Investigaciones Fisicoquímicas Teóricas y Aplicadas, Facultad de Ciencias Exactas, Universidad Nacional de La Plata, La Plata 1900, Argentina*
[c] *Department of Biosciences and Oral Diagnosis, Universidade Estadual Paulista (Unesp), Institute of Science and Technology (ICT), São José dos Campos, São Paulo, Brazil*

ARTICLE INFO

Keywords:
Photodynamic therapy
Photodithazine®
Gram-positive bacteria
Methicillin-resistant *Staphylococcus aureus* (MRSA)
Chlorine
Galleria mellonella

ABSTRACT

Staphylococcus aureus infections are a severe health problem due to the high mortality rate. Conventional treatment of these infections is *via* the administration of antibiotics. However, its indiscriminate use can select resistant microorganisms. Thus, it is necessary to develop alternatives for antibiotic therapy. Antimicrobial Photodynamic Therapy (aPDT), a therapeutic method that associates a photosensitizer (PS), a light source with adequate wavelength to the PS, interacts with molecular oxygen generating reactive oxygen species responsible for cell inactivation, is a viable alternative. This work aimed to analyze, *in vitro* and *in vivo*, the action of aPDT with PS Photodithazine® (PDZ) on the methicillin-resistant *S. aureus* (MRSA) strain. In the *in vitro* method, the *S. aureus* biofilm was incubated with PDZ at 50 and 75 $\mu g.mL^{-1}$ for 15 min, adopting the light dose of 25, 50, and 100 J/cm^2. In addition, PS interaction, formation of reactive oxygen species (ROS), bacterial metabolism, adhesion, bacterial viability, and biofilm structure were evaluated by scanning electron microscopy. Subsequently, the strain was inoculated into models of *Galleria mellonella*, and the survival curve, health scale, blood cell analysis, and CFU/mL of *S. aureus* in the hemolymph were analyzed after aPDT. In the *in vitro* results, bacterial reduction was observed in the different PDZ concentrations, highlighting the parameters of 75 $\mu g.mL^{-1}$ of PDZ and 100 J/cm^2. As for *in vivo* results, aPDT increased survival and stimulated the immune system of *G. mellonella* infected by *S. aureus*. aPDT proved effective in both models, demonstrating its potential as an alternative therapy in treating MRSA bacterial infections.

1. Introduction

Staphylococcus aureus is responsible for several infections, from boils to sepsis, which can cause death [1]. The conventional treatment is carried out by administering antibiotics. However, indiscriminate use is responsible for the emergence of resistant bacteria. Strains of *S. aureus* resistant to several antibiotics have already been described, the most clinically important being methicillin-resistant *Staphylococcus aureus* (MRSA) [2].

The Center for Disease Control and Prevention (CDC) identified in 2019 that the rate of MRSA strains exceeded 41% among adults and 28% among pediatric patients, with approximately 323,700 cases and reaching about 10,600 deaths, resulting in 1.7 billion dollars in expenses [3]. These high mortality rates in hospitalized patients have caused worldwide concern.

In 2017, a list of the 12 bacteria most at risk to human health due to their high resistance was divided into three categories of urgency, in which MRSA was reported as a high priority [4]. In 2019, WHO reinforced the alert about the shortage of developing new antibiotics for MRSA. Currently, only seven antibiotics are in the preclinical phase for

* Corresponding authors.
E-mail addresses: agminan@inifta.unlp.edu.ar (A.G. Miñán), juguerra@univap.br (J.G. Pinto), juliana.junqueira@unesp.br (J.C. Junqueira), juferreira@univap.br (J. Ferreira-Strixino).

https://doi.org/10.1016/j.jphotobiol.2024.112860
Received 25 October 2023; Received in revised form 15 January 2024; Accepted 1 February 2024
Available online 3 February 2024

treating these infections, but with no prediction of applicability, reinforcing the importance of alternatives to antibiotic therapy [4]. Among these alternatives, antimicrobial photodynamic therapy (aPDT) stands out due to its effectiveness and not generating antimicrobial resistance.

The aPDT comprises the association of a photosensitizer (PS), which, after interacting with the cell, is excited by light with a wavelength appropriate to that PS, reacting with molecular oxygen and forming reactive oxygen species (ROS), responsible for cell inactivation [5–7]. ROS can cause bacterial cell death instead of inhibiting their growth, reducing the chances of microorganisms developing tolerance or resistance to aPDT [7]. Photodithazine® (PDZ) is an e6 chlorin of Russian origin, obtained from the cyanobacterium *Spirulina platensis*, demonstrating a high ROS production when irradiated [8,9].

Therefore, additional studies are needed to evaluate the application of aPDT with PDZ, both *in vitro* and *in vivo*, as an alternative to antibiotic therapy. Invertebrate models for *in vivo* research stand out due to the ease of handling and the size of the larvae, allowing the injection of substances directly into the hemolymph, which will be collected to be analyzed. In addition, they have an innate immune system with the action, mainly, of hemocytes with a similar function to the neutrophils of mammals, as is the case of the species *Galleria mellonella*, thus allowing us to understand both the effect of the bacteria in the organism and the impact of the action of aPDT with PDZ in MRSA strains [10–12]. It is important to emphasize that invertebrate models have limitations and do not reflect the complexity of mammalian systems. However, carrying out studies in invertebrates beforehand leads to a decrease in the use of animals for further study in mammals. This study aimed to assess the impact of PDZ-mediated aPDT on multiresistant *Staphylococcus aureus* (MRSA) through two stages: i) *in vitro* testing to determine its effectiveness in inactivating mature biofilms with a high density of sessile cells to mimic the challenge of eliminating a biofilm in the absence of the immune system, as in industrial biofouling; and ii) *in vivo* testing, to assess the effectiveness of aPDT in treating MRSA infection in larvae of *Galleria mellonella*, which serve as an *in vivo* model possessing an immune system. The findings from this work will aid in determining the applicability of general or specific aPDT conditions for eliminating biofilms on abiotic surfaces or those related to bacterial infection.

2. Methodology

2.1. In vitro Tests

2.1.1. Maintenance and Preparation of Bacterial inoculum

A multidrug-resistant strain of *S. aureus*, MRSA strain (PBNS02SA), from the bacteria collection of the Laboratory of Photobiology Applied to Health (PhotoBioS Lab) was used in this study. The stock culture of this strain was maintained at −20 °C in brain heart infusion broth (BHI, Thermo Fisher Scientific™) that contained 5% (*v*/v) glycerol. Subsequently, the MRSA strain was inoculated in BHI and grew overnight at 37 °C. After incubation, the MRSA suspension (planktonic cells) was adjusted to 10^8 colony-forming units (CFU).mL-1 in fresh BHI broth. The viable count method confirmed the number of cells in the bacterial suspension.

2.1.2. Obtaining and Preparing the Photosensitizer

Photodithazine is a chlorin-e6 bis-*N*-methylglucamine salt. The photosensitizer was produced by the Russian company Veta-Grand® (Moscow, Russia) and provided by the Biophotonics Laboratory of the Institute of Physics of São Carlos – USP. PDZ is a mixture of di-*N*-methyl-D-glucosamine complexes of Chl e6 (60%), Chl p6, and purpurins 7 and 18, according to a study by Uzdensky, 2003 [13]. According to Pires et al. 2014, Photodithazine is a commercial water-soluble glucosamine salt of chlorine(e6), with chlorine e6 being derived from chlorophyll oxidation [14].The 5 mg.mL^{-1} stock solution was diluted in Phosphate Buffered Saline (PBS) at 50 and 75 μg.mL^{-1} working concentrations. PDZ was stored at 4 °C and kept in the dark during the process. The concentrations were determined based on a previous study, which demonstrated total bacterial inactivation in planktonic strains of MRSA [15].

2.1.3. Biofilm Preparation

The biofilm was grown on 24-well plates[16]. Briefly, MRSA suspensions (1×10^8 cells.mL^{-1}) were prepared as described above and then diluted 1:10 in fresh BHI broth. Aliquots (2 mL) of this bacterial suspension (1×10^7 cells.mL^{-1}) were added to the wells of sterile flat-bottom 24-well assay plates and incubated at 37 °C for 48 h to allow biofilm formation with a change to fresh medium after 24 h. After the tests, the viable bacteria in the biofilm were enumerated using the plate counting method after their mechanical detachment.

2.1.4. Interaction of Photodithazine® in the Biofilm of MRSA Strains

PDZ interaction was studied in biofilms formed on coverslips in a 24-well plate according to the above protocol. The 48 h biofilm coverslips were exposed to PDZ at 50 and 75 μg.mL^{-1} concentrations and incubated for 15 min at 37 °C in the dark. Then, the photosensitizer was removed, and the samples were fixed in 4% paraformaldehyde and washed with PBS. Finally, 48 h-biofilms coverslips were mounted on a slide with ProLong™ Diamond Antifade Mountant with DAPI (4′,6-diamidino-2-phenylindole) - Thermo Fisher Scientific ™ and analyzed in a Zeiss LSM 700 Confocal Microscope with excitation for DAPI at 405 nm and PDZ at 555 nm.

2.1.5. Application of aPDT and Division of Experimental Groups

The antimicrobial effect of aPDT against the 48 h biofilm of MRSA was evaluated with PDZ. PDZ at 50 and 75 μg.mL^{-1} were added to 48 h biofilms and incubated in the dark for 15 min. After incubation, the biofilms were irradiated with light doseof 25, 50, and 100 J/cm^2 (Biotable Biopdi660 with 54 LEDs with a wavelength of 660 nm, 25 mW/cm^2). Finally, the aPDT-treated biofilm wells (aPDT group) were washed with PBS and broken with a platinum loop. The sample was then diluted and seeded on BHI plates for colony-forming unit counting. The results were expressed in a logarithmic scale ($\log_{10}$). In addition, control assay experiments were performed with 48 h-biofilms in triplicate series and with three replicates as follows:

i) Non-irradiated control group, biofilms were only incubated in fresh BHI broth; ii) Irradiated control group, biofilms were incubated in fresh BHI broth and irradiated without photosensitizer, and iii) PDZ group biofilms were kept in darkness after addition of PDZ at the specified concentrations.

From the results obtained, 75 μg.mL^{-1} and 100 J/cm^2 parameters were selected for applying aPDT in the other tests.

2.1.6. Quantification of Biomass

The disruptive effect of aPDT against 48 h biofilm of MRSA was evaluated at 75 μg.mL^{-1} of PDZ and a light doseof 100 J/cm^2. Total biofilm biomass was quantified using crystal violet (CV). After treatment with aPDT, the wells were washed with PBS, and the samples were fixed with methanol (Sigma Aldrich™) for 15 min. Then, methanol was removed, and the biofilm samples were dried at 37 °C. After drying, 0.5% crystal violet (CV) – Sigma Aldrich™ was added to the samples and incubated for 20 min. Subsequently, the groups were washed twice with PBS to remove the CV that had not adhered to the biofilm. The CV, which remained attached to the biofilm, was released by adding acetic acid (33%) Sigma Aldrich™. Finally, the CV solutions were quantified at an absorbance of 560 nm with a PACKARD spectrophotometer reader, model Perkin Elmer SpectraCount BS 10000.

2.1.7. Analysis of Reactive Oxygen Species Production

ROS production was quantified using the 2′, 7′-dichlorodihydrofluorescein (DCFDA) diacetate probe (Thermo Fisher Scientific™). After diffusion into the cell, it is deacetylated by cellular esterases to a non-fluorescent compound (DCFH) and subsequently oxidized by reactive

oxygen species to 2′, 7′-dichlorofluorescein (DCF, a fluorescent compound), which is used to quantify ROS production after aPDT. Only the irradiated control group and the biofilms subjected to aPDT were evaluated in this assay. After aPDT treatment of 48 h biofilms, the PDZ was removed, and DCFDA reagent was added at a concentration of 100 μM, incubated for 30 min, and then irradiated at 100 J/cm^2. Fluorescence measurements were performed using the Synergy HT Multi-Detection Microplate Reader (Bio-Tek, Winooski, VT, USA) with excitation at 480 nm and emission at 530 nm.

2.1.8. Evaluation of Metabolic Activity

The metabolic activity was quantified using the reagent Resazurin - Sigma Aldrich™, whereby viable bacteria can reduce resazurin to resorufin. The resazurin was prepared with PBS in a stock solution of 6.8 mg.mL^{-1}. The metabolic activity of biofilms-wells exposed to aPDT was achieved by adding 4 μL resazurin to each well. After 4 h incubation at 37 °C, resazurin conversion was quantified by fluorescence spectroscopy using the Synergy HT Multi-Detection Microplate Reader (Bio-Tek, Winooski, VT, USA) at 528/20 nm excitation and 645/40 nm emission.

2.1.9. Biofilm Structural Evaluation by Scanning Electron Microscopy (SEM)

Biofilms were grown on coverslips in 24-well plates and subjected to aPDT (75 μg.mL^{-1} PDZ and 100 J/cm^2 light dose) as described above. After applying the therapy, the biofilms (including the control groups) were fixed. Then, the samples were dehydrated with increasing alcohol solutions of 10, 25, 70, and 90% for 20 min and 100% for 1 h. For analysis with the scanning electron microscope (EVO MA 10 Zeiss), the biofilm samples were dried at the critical point and metalized with a 20 nm gold layer (Emitech K550x Metallizer).

2.2. In vivo Tests

2.2.1. Invertebrate Model Selection of Galleria mellonella and Infection in vivo

For *in vivo* MRSA infection, *G. mellonella* larvae provided by the Microbiology and Immunology laboratory of the Institute of Science and Technology of São José dos Campos - UNESP were used. Ten larvae were used for each group, infected in the final stage of development with body weight between 200 and 250 mg. The selected insects had a light coloration, without dark pigments in their cuticle, ruling out the possibility of an infectious process in the animal interfering with the results.

The infection in the animal was performed according to the methodology established by Junqueira et al. 2012 [11]. Injections were applied with the *S. aureus* suspension into the insect's hemolymph *via* its last right proleg. To evaluate the MRSA inoculum for *in vivo* aPDT assays, a *G. mellonella* survival curve was performed by injecting larvae with 10,^{4} 10^5, and 10^6 CFU per larva from *S. aureus* suspensions, and 10^5 was selected for application of the aPDT test due to the better results. The control group was injected with 10 μL of PBS to assess the impact of the trauma of the injections or the operator's manipulation technique, excluding physical damage during the injection. After the injection, the larvae were stored in plastic containers in the dark at 37 °C.

Once the inoculum concentration for the *in vivo* assay was established, PS concentrations and light doseswere tested, as detailed in the following sections.

2.2.2. Standardization of Parameters: PDZ Concentration and Light Dose

Different light doses and PDZ concentrations were tested to define the working parameters. This standardization is described in the supplementary material. Briefly, light doses of 10, 25, 50, 75, and 100 J/cm^2 (30 mW/cm^2) were initially applied at a wavelength of 660 nm. For *in vitro* assays, PDZ concentrations of 25, 50, 75, and 100 μg.mL-1 were used, while for *in vivo* assays, concentrations of 2.5 × 10–7, 0.25, 5 μg.mL-1 and light dose of 10 J/cm^2 were tested. The 10 J/cm^2 light dose and 5, 0.25, 2.5 × 10–7 μg.mL-1 concentrations were selected.

2.2.3. Antimicrobial Photodynamic Therapy in Galleria mellonella Model

In vivo aPDT assays were performed on *G. mellonella* infected with MRSA at selected PDZ concentrations of 5, 0.25; 2.5 × 10^{-7} μg.mL^{-1}, in the volume of 10 μL were administrated a dose of 5 × 10^{-2}, 2.5 × 10^{-3}, 2.5 × 10^{-9} μg of PDZ, respectively. The irradiation was performed at a light doseof 10 J/cm^2, and the groups were divided as described in Table 1. One with only the injection of PBS, one with the injection of PBS and MRSA, a group subjected only to irradiated (L); one with only the injection of PDZ and without irradiation, and a PDT group with the application of PDZ and subjected to irradiation. (Table 1).

After 30 min of *G. mellonella* infection, the groups received PDZ or PBS concentrations (10 μL) in the left *proleg* and were incubated for 15 min for PDZ interaction. Then, each larva was placed in a well of the 24-well plate, and the irradiated groups were exposed to light. The other groups were kept in the dark. After irradiation, the animals were placed in plastic larval containers in the dark at 37 °C. The number of dead larvae was recorded daily to determine the survival curve for seven days or until the complete death of the aPDT group.

2.3. Health and Survival Scale

The health and survival scale of *G. mellonella* was evaluated during the survival curve analysis after applying aPDT. The scale was based on the study by Loh et al. (2013) [17], in which a pathological scoring system was established to evaluate subtle differences in larval health based on appearance, observing activity (animal movement), cocooning ability, presence of melanization, and survival. A score was assigned to each trait, as shown in Fig. 1, and the sum of the scores, ranging from 0 to 10, was calculated at the end. All larvae were initially selected for the test with a health scale equal to 10.

2.3.1. Hemocyte Analysis

For hemocyte analysis, *S. aureus* was inoculated into *G. mellonella* at a concentration of 10^5 bacteria/mL after exposure to aPDT. The larvae were incubated at 37 °C for 30 min. The division into groups is described in Table 2. For each group, 10 larvae per group were used.

Hemolymph collection was performed by immobilizing the larvae in Petri dishes. The animals were then cut ventrally in a cephalocaudal direction with a scalpel and squeezed to remove the hemolymph. 10 μL of hemolymph were collected and diluted in 990 μL of IPS buffer (2% NaCl; 0.1 M glucose; 30 mM sodium citrate; 26 mM citric acid, and 10 mM EDTA) arranged in previously frozen Eppendorf tubes. The hemocyte count was performed in Neubauer chambers.

2.3.2. Hemolymph Viable S. aureus Cell Count

The number of bacteria in the hemolymph (expressed as colony-forming units per mL, CFU/mL) was used to assess the persistence of *S. aureus* in *G. mellonella* after aPDT treatment. Hemolymph was collected after 30 min of treatment as previously described. Then, the solution was serially diluted in PBS and plated on BHI agar by the drip method. After 24 h, the CFU/mL count was carried out, and the results were expressed as $\log_{10}$.

2.4. Statistical Analysis

The *in vitro* and *in vivo* assays were performed in triplicate of three

Table 1
G. mellonella in vivo experimental groups, location and content of injections.

Group	Right *Proleg*	Left *Proleg*	Light
PBS (Control)	PBS	PBS	–
MRSA (Control)	MRSA	PBS	–
L (light dose)	MRSA	PBS	X
PDZ	MRSA	PDZ	–
aPDT	MRSA	PDZ	X

Category	Description	Score
Activity	No activity	0
	Minimal activity on stimulation	1
	Active when stimulated	2
	Active without stimulation	3
Cocoon formation	No cocoon	0
	Partial cocoon	0.5
	Full cocoon	1
Melanization	Complete melanization (black)	0
	Dark spots on brown wax worm	0
	≥3 spots on beige wax worm	2
	<3 spots on beige wax worm	3
	No melanization	4
Survival	Dead	0
	Alive	2

Fig. 1. Health scale used for the initial selection of larvae. Score attributed to each characteristic of the larvae [17].

Table 2
G. mellonella in vivo experimental groups for hemocyte analysis, location, and injection content.

Group	Right *Proleg*	Left *Proleg*	Light
PBS Control	PBS	PBS	–
PBS (L10*) Control	PBS	PBS	X
PBS (PDZ) Control	PBS	PDZ	–
PBS (PDZ + L10*) Control	PBS	PDZ	X
MRSA Control	MRSA	PBS	–
L (light dose)	MRSA	PBS	X
PDZ	MRSA	PDZ	–
aPDT	MRSA	PDZ	X

* L10: irradiation at 10 J/cm^2.

independent experiments. In the *in vitro* and *in vivo* experiments, health scale, hemocyte analysis, and CFU/mL of hemolymph, the results were statistically analyzed using the Bioestat 5.0 software, with ANOVA One way and Tukey. For the *in vivo* larval survival experiments, statistical analysis was performed with the Logrank test using GraphPad Prism software.

3. Results

3.1. Interaction of Photodithazine® in the Biofilm of MRSA Strains

To evaluate the interaction of the PDZ with the biofilm, fluorescence confocal microscopy, as presented in Fig. 2. DAPI binding to the genetic material allowed visualization of the bacterial morphology in cocci arrays characteristic of *Staphylococcus spp.* PDZ fluorescence at concentrations of 50 and 75 μg.mL^{-1} allowed us to visualize the whole bacterial morphology, and the confocal observation indicated its interaction and that the incubation time of 15 min was sufficient for PDZ to interact with biofilm. The 3D image shows the PDZ in the bacteria cytoplasm.

3.2. Photodynamic Inactivation of Mature MRSA Biofilms

The group treated only with PDZ showed no significant difference from the non-irradiated control, demonstrating no toxicity at 50 and 75 μg.mL-^{1}. Also, the control groups were irradiated at light doses at concentrations of 100, 50, and 25 J/cm^2 and showed no significant differences from the dark group. Biofilms treated with aPDT presented a reduction between 4 and 6 logs on viability compared with the PDZ 50 and 75 μg.mL^{-1} control, demonstrating that the therapy's potential (Fig. 3A). There was a significant difference between the non-irradiated control group and all aPDT groups ($p < 0.01$), with emphasis on the parameters of 100 J/cm^2 combined with 50 and 75 μg.mL^{-1} PDZ presenting reductions of 6.4 and 6.7 log10, respectively. A significant difference ($p < 0.01$) was observed between PDT treatments with 25 J/cm^2 and 50 J/cm^2 and PDT with 100 J/cm^2, with the latter protocol being the most efficient. Therefore the parameters of PDZ concentration of 75 μg.mL-1 and light dose of 100 J/cm^2 were selected for further studies.

3.2.1. Quantification of Biofilm Biomass After aPDT

There was no significant difference between all the groups evaluated, meaning that the therapy could not disrupt the total biofilm biomass compared to the non-irradiated control group. Nevertheless, the absence of a significant difference between the absorbances means that the structure formed in all groups was similar, and the construction of the biofilm in all groups was homogeneous (Fig. 3B).

3.2.2. Analysis of the Production of Reactive Oxygen Species (ROS)

It was possible to observe a significant difference ($p \leq 0.01$) between the irradiated control group and the aPDT group. The substantial increase in ROS production of about 1140 a.u. is related to the interaction of PDZ with light, demonstrating the potential of aPDT for ROS production and biofilm inactivation (Fig. 3C), justifying the reduction in viability after aPDT.

3.2.3. Evaluating Bacterial Metabolic Activity After aPDT

Bacterial metabolic activity was evaluated using the resazurin reagent. The fluorescence reading showed that the non-irradiated control and irradiated group and only the PDZ group obtained higher metabolic activity. In contrast, the aPDT group showed low metabolic activity in the aPDT group, compatible with the observed bacterial reduction in CFU/ml count.

The PDZ, non-irradiated, and irradiated control groups did not significantly differ from the non-irradiated control group. This confirms that PDZ without irradiation did not affect bacterial metabolism. However, all control groups (non-irradiated, irradiated, and PDZ groups) showed significant differences from the aPDT group ($p \leq 0.01$), indicating that photodynamic therapy significantly alters bacterial metabolism and damages biofilm cells (Fig. 3D).

3.2.4. Biofilm Structural Evaluation by Scanning Electron Microscopy (SEM)

The SEM analysis shows the cocci morphology characteristic of *S. aureus* in the biofilm structure in all groups (Fig. 4). In the non-irradiated control, grouped bacteria with extracellular matrix and overlapping layers were observed, characterizing biofilm formation. The irradiated control group showed slightly reduced bacteria, while the PDZ group (75 μg.mL^{-1}) showed biofilm formation similar to the non-irradiated control group. The aPDT group showed a qualitative decrease in bacterial attachment after aPDT treatment at both observed magnifications (2.00kx).

3.3. in vivo Model

3.3.1. Determination of Tested Parameters

Tests were carried out to standardize the MRSA inoculum in *Galleria mellonella*, selecting a concentration of 10^5 CFU per larva, PDZ concentrations of 5; 0.25 and 2.5 × 10^{-7} μg.mL^{-1} and irradiated at a t light dose of 10 J/cm^2.

3.3.2. Antimicrobial Photodynamic Therapy (aPDT)

In vivo aPDT assays were performed on *G. mellonella* infected with MRSA at PDZ concentrations of 5, 0.25; 2.5 × 10^{-7} μg.mL^{-1}, using irradiation at a light dose of 10 J/cm^2.

Therefore, it was observed that the CTRL-PBS group achieved 100%

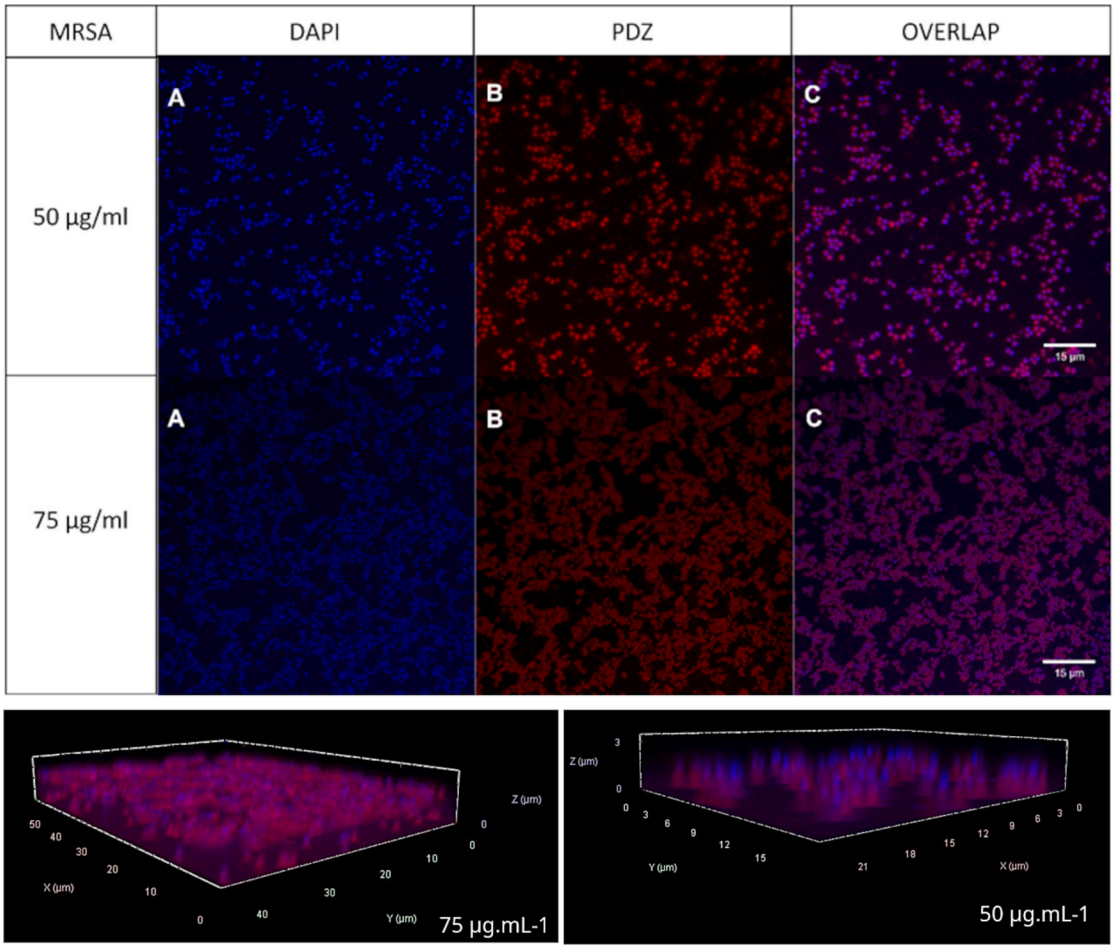

Fig. 2. Micrograph obtained by fluorescence Confocal Microscopy of MRSA strain incubated with PDZ at 50 and 75 µg.mL^{-1}, and a 3D image of the interaction with PDZ in both concentrations. Labeling with DAPI. Fluorescence emitted by the PDZ. Channel overlap.

survival up to 168 h (7 days), demonstrating that the manipulation of the larvae did not affect mortality (Fig. 5).

The CTRL MRSA group exhibited 60% survival within 24 h, 20% within 72 h, and lethality within 96 h. The PDZ and L 10 J/cm^2 groups had survival rates similar to the CTRL MRSA group, indicating that mortality was identical regardless of light application or PDZ concentration, indicating that larval death was due to infection by MRSA.

The survival of the aPDT 2.5 × 10^{-7} µg.mL^{-1} group was similar to that of the CTRL MRSA group, demonstrating that the action of aPDT on these parameters did not influence the survival of the larvae, with no significant differences between the groups. The aPDT 5 µg.mL^{-1} group had a more prolonged survival (20*h*) than the CTRL MRSA group. The aPDT 0.25 µg.mL^{-1} group, on the other hand, showed lower mortality compared to the MRSA control group, helping the survival of the larvae in 90% in 24 h and 40% in up to 168 h, not showing total mortality in 7 days, obtaining significant differences compared to the CTRL MRSA group, demonstrating the potential of PDZ therapy to inactivate the microorganism without causing more significant damage to the host.

3.3.3. Health and Survival Scale, Hemolymph Analysis, and CFU/mL of Hemolymph

The health scale (Fig. 6) after the application of the therapy with PDZ concentrations of 5, 0.25, 2.5 × 10^{-7} µg.mL^{-1} and light doseof 10 J/cm^2, shows that the health index of the CTRL PBS and L 10 J/cm^2 groups were around 10, did not reduced the health index.

The CTRL MRSA and PDZ groups showed similar health scales with minimal variations from 4.5/3 to 1.5/0 within 48 h. The MRSA control group achieved a health index of about 4 at 24 h but decreased to 0 at 96 h. The PDZ group at concentrations of 0.25 and 2.5 × 10^{-7} µg.mL^{-1} presented indexes of 3 and 4 but decreased to 0 in 48 h. The PDZ 5 µg.mL^{-1} group obtained an index of 4.5 at 24 h and 0 at 96 h, demonstrating that the health of the larvae in the concentration of 5 µg.mL^{-1}, was slightly better than in the other groups PDZ, but without significant difference with the control group.

The health indexes of the aPDT with 2.5 × 10^{-7} µg.mL^{-1} and 5 µg.mL^{-1} of PDZ were similar to those of the CTRL MRSA group, reaching indexes of approximately 2 and 3 at 24 h, and index 0 at 96 and 120 h, respectively. However, the aPDT group with 0.25 µg.mL^{-1} of PDZ brought higher rates than the CTRL MRSA group, demonstrating that the action of the therapy improved the health of the larvae.

Based on the results obtained in previous experiments, a concentration of 0.25 µg.mL^{-1} of PDZ and a light doseof 10 J/cm^2 were selected for applying aPDT and subsequent hemocyte counting.

The hemocyte count (Fig. 5B) showed that all the PBS control groups [CTRL PBS, CTRL PBS (L10), CTRL PBS (PDZ), and CTRL PBS (PDZ + L10)] did not show significant differences among themselves, demonstrating that the effect of light alone, PDZ alone at a concentration of 0.25 µg.mL^{-1} and the combination of PDZ and light did not influence the increase in hemocytes.

The CTRL PBS group did not show significant differences from the CTRL MRSA group, suggesting that the MRSA strain could not induce an adequate immune response in the larvae. However, the CTRL MRSA group obtained significant differences from the irradiated CTRL MRSA group (L10), exhibiting that the action of light combined with the presence of MRSA bacteria induced a decrease in the production of hemocytes.

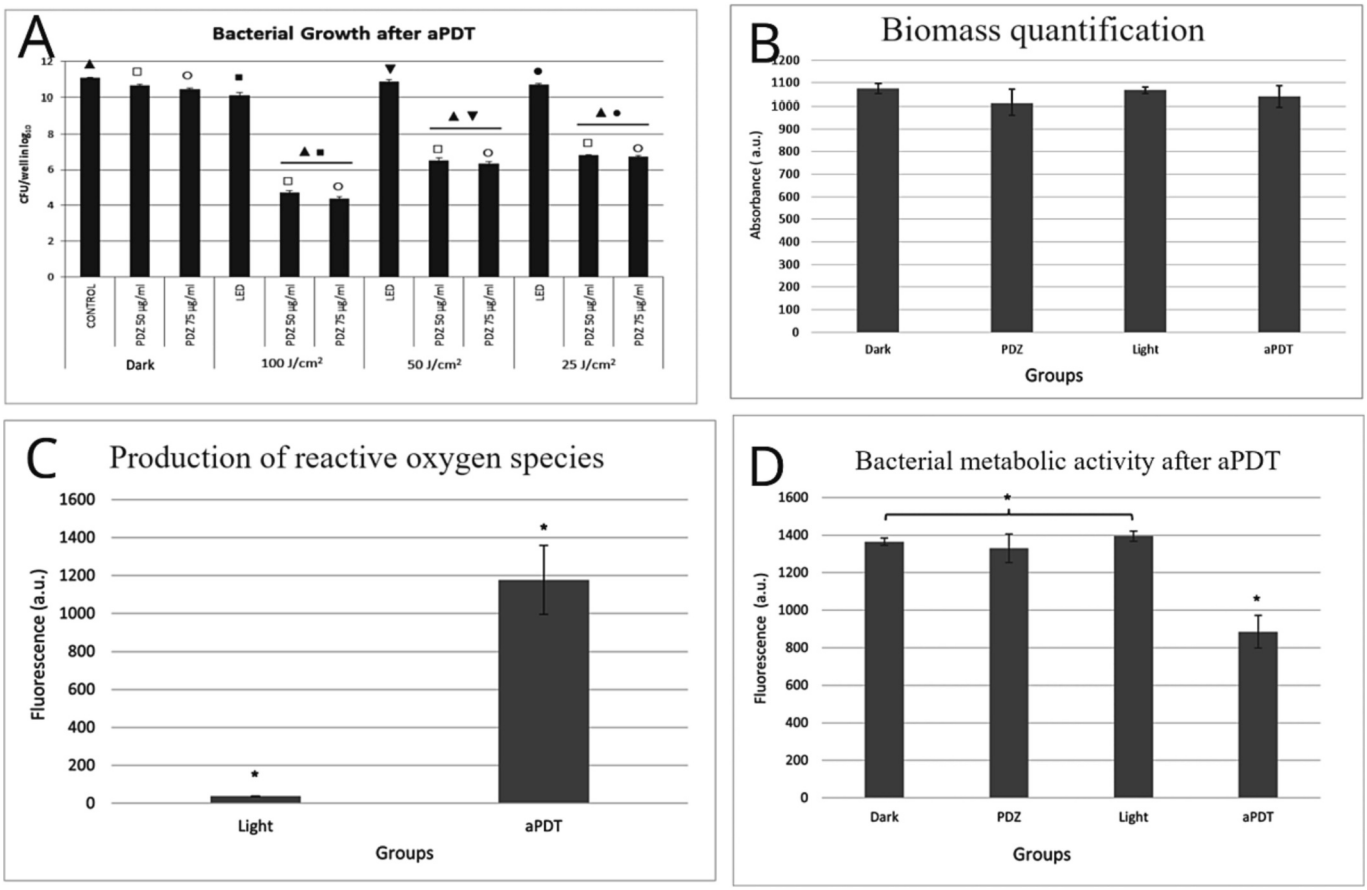

Fig. 3. (A) Mean values of CFU/well in $\log_{10}$ in MRSA biofilm, showing non-irradiated and irradiated control group, PDZ at concentrations of 50, 75 $\mu g.mL^{-1}$ non-irradiated and irradiated at 100, 50, 25 J /cm^2 light doses. Icons *, ○,◇, and □ represent statistical differences between groups. (B) Biomass quantification by crystal violet staining method. Shown are the non-irradiated control group, non-irradiated PDZ 75 $\mu g.mL^{-1}$ group, control group irradiated at 100 J/cm^2, and aPDT group with PDZ 75 $\mu g.mL^{-1}$ irradiated at 100 J/cm^2. (C) ROS production in MRSA biofilm, showing the irradiated control group and the aPDT group with a concentration of 75 μgmL^{-1} of PDZ, both irradiated at a light dose of 100 J/cm^2. The (*) symbols indicate the statistical difference between the groups. (D) Evaluation of bacterial metabolic activity with resazurin in arbitrary units of fluorescence in MRSA biofilm, showing non-irradiated and PDZ (75 $\mu g.mL^{-1}$) control groups, and also irradiated control and aPDT groups, the latter both irradiated at light dosesof 100 J/ cm^2. (For interpretation of the references to colour in this figure legend, the reader is referred to the web version of this article.)

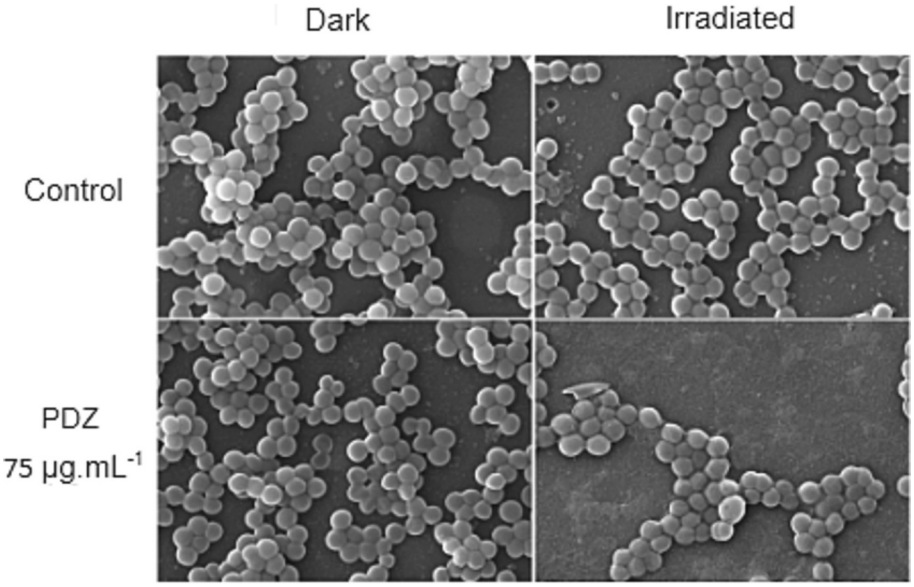

Fig. 4. – Micrograph obtained by biofilm scanning electron microscopy, at 2000× magnification of the non-irradiated control, irradiated control (100 J/cm^2), PDZ (75 $\mu g.mL^{-1}$), and aPDT groups.

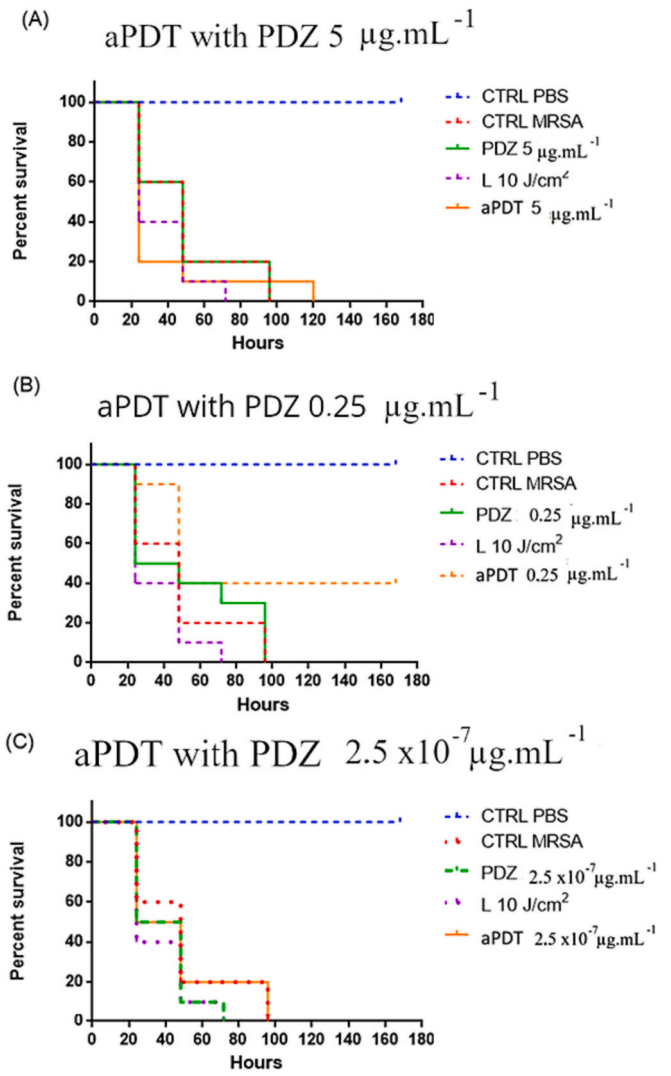

Fig. 5. Survival test after application of aPDT with PDZ in *G. mellonella*, showing the non-irradiated PBS control group, L Group irradiated with 10 J/cm^2, MRSA control, PDZ group, and aPDT. Fig. (A) – shows the concentration of PDZ 5 µg.mL^{-1}. (B) 0.25 µg.mL$^{-1,}$ and (C) 2.5 × 10^{-7} µg.mL^{-1}. Comparison of survival curves by Log-rank test: Fig. A:- There are statistically significant between the groups "CTRL MRSA" and "CTRL PBS" (⟨0,0001), and no statistically significant differences were found in the groups "CTRL MRSA" with group "PDZ" (p = 1,0000), "L" (p = 0,1975) and "aPDT" (p = 0,4303). Fig. B:- There are statistically significant between the groups "CTRL MRSA" and "CTRL PBS" (<0,0001), and no statistically significant differences were found in the groups "CTRL MRSA" and "PDZ" (p = 0,7705), "L" (p = 0,1975) and "aPDT" (p = 0,0318). Fig. C:- There are statistically significant between the groups "CTRL MRSA" and "CTRL PBS" (<0,0001), and no statistically significant differences were found in the groups "CTRL MRSA" and "PDZ" (p = 0,2932), "L" (p = 0,1975) and "aPDT" (p = 0,8219).

The CTRL PBS group did not obtain significant differences concerning the CTRL MRSA group (PDZ 0.25 µg.mL^{-1}), suggesting that the interaction of PDZ with the MRSA strain did not influence the increase in the immune response. However, in the presence of light, the CTRL MRSA group (PDZ 0.25 µg.mL^{-1}) obtained significant differences with the aPDT 0.25 µg.mL^{-1} group, meaning that the application of the therapy favored the production of hemocytes (Fig. 5B).

In addition, the aPDT 0.25 µg.mL^{-1} group also obtained significant differences with the CTRL PBS and CTRL MRSA groups, demonstrating that the application of the therapy increased the production of hemocytes compared to the immune response produced only in the presence of the bacteria.

The absolute values of CFU/mL were expressed on the log10 scale (Fig. 5C). The CTRL PBS group showed a slight bacterial presence, a natural characteristic of the *G. mellonella* species. The groups exposed to MRSA infection maintained around 6 $\log_{10}$ regardless of the application of light or PDZ alone. Thus, they obtained a significant difference with the CTRL PBS group, demonstrating the established infection. Finally, a slight bacterial reduction was observed when the MRSA-infected larvae received the aPDT treatment, but not significant to CTRL MRSA.

4. Discussion

In the present work, the efficacy of aPDT treatment was first evaluated using an *in vitro* biofilm model of a multidrug-resistant *S. aureus* (MRSA) strain. Furthermore, a second approach focused on antimicrobial therapy applied to control MRSA infection using the *in vivo Galleria mellonella* model. Here, we also evaluated whether or not the *in vitro* aPDT parameters could be applied to *the in vivo* model.

First, the efficacy of aPDT in mature biofilms was evaluated using a multidrug-resistant strain of *S. aureus* (MRSA) grown for 48 h in a BHI medium, which favors biofilm development, maturation, and biomass formation, compared to other culture media. The 48 h mature biofilms are also more difficult to inactivate by antimicrobial agents than early biofilms [18,19]. Although in previous work, the effect of aPDT (PDZ concentrations of 75 and 100 µg.ml-^{1} irradiated at light dosesof 25, 50, and 100 J/cm^2) achieved the eradication of the planktonic cells of MSSA (methicillin-sensitive *S. aureus*) and MRSA strains [15], the present mature biofilm model was more tolerant to the aPDT. Therefore, mature biofilms represent a challenge to antimicrobial treatments, including aPDT, due to both the structure and resistance factors of the MRSA strain, such as efflux pumps, which are capable of eliminating antimicrobials and PS [20]. For these reasons, in this work, the mature biofilm model established for aPDT assays exhibited an amount of sessile cells and biomass superior to that found in infected indwelling devices or prostheses to challenge aPDT based on the photosensitizer PDZ under extreme conditions.

4.1. PDZ Interaction and Bacterial Metabolic Activity After aPDT of Mature MRSA Biofilms

The interaction of PDZ has been observed in planktonic strains but has not been studied in sessile cells, making it necessary to follow this interaction in the structure of the biofilm. Although the interaction of compounds in bacterial cells is a much-debated issue, it is known that the more complex composition of Gram-negative bacteria can hinder the entry of compounds compared to Gram-positive bacteria, which have a porous layer of peptidoglycan [21,22]. Previous studies have evaluated the interaction of methylene blue (MB) (100 µg.mL^{-1}) in planktonic strains of Gram-negative and Gram-positive bacteria, with less interaction observed in Gram-negative bacteria and greater interaction in Gram-positive ones [23,24]. This difficulty in the interaction of PS in Gram-negative planktonic bacteria, which is mainly due to the composition and structure of the membrane, can be increased in the biofilm since the production of an extracellular matrix involves the bacteria in the protection of their cell membrane. This study demonstrated that the 15-min incubation period was sufficient for the interaction of the PDZ into the different layers of the biofilm, as observed in the 2.5D micrographs, which is an essential factor for the success of aPDT. However, complete inactivation of the MRSA biofilm was not achieved despite the application of the same parameters (PDZ at concentrations of 50 and 75 µg/ml and light dose of 50 and 100 J/cm^2) as previously used in planktonic culture, probably due to the complex structure of the biofilm, composed of layers of bacteria attached to the cell matrix, with the combined action of several virulence factors, such as surface components, adhesion molecules, toxins, and immune evasion molecules, making it difficult to eliminate the infection [25]. Although complete inactivation was not achieved in the present study, a reduction of up to

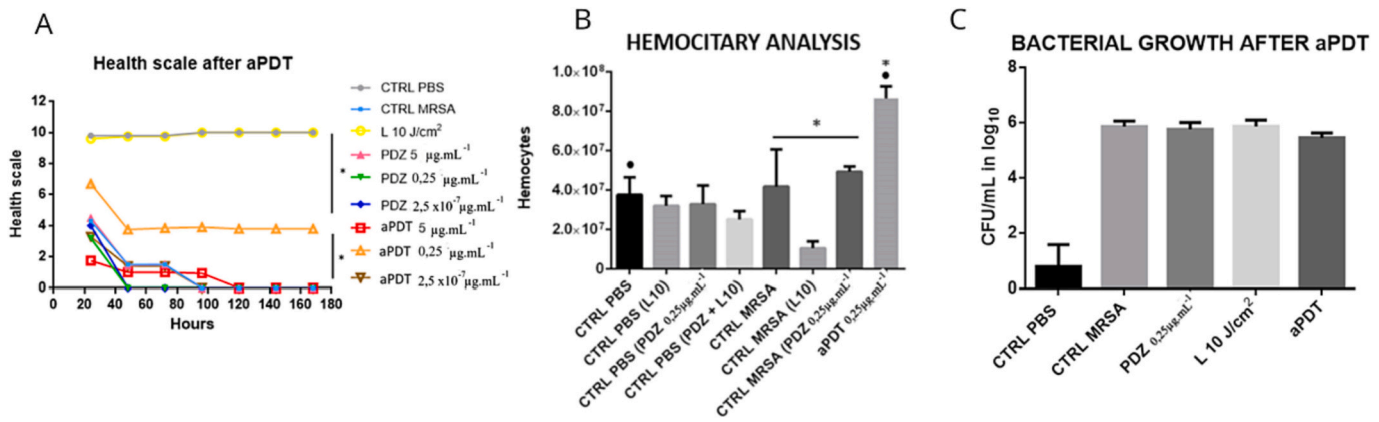

Fig. 6. (A) *G. mellonella* health scale after aPDT, the control groups (PBS, not irradiated and irradiated) at 10 J/cm^2, Control MRSA, only PDZ 5; 0.25; 2.5 × 10^{-7} µg.mL^{-1}, only L 10 J/cm^2 and aPDT 5; 0,25; 2.5 × 10^{-7} µg.mL^{-1} with a light dose of 10 J/cm^2. The (*) icon shows the statistical difference between groups. (B) Hemocytic count of *G. mellonella* after aPDT, showing the group Control PBS non-irradiated, Control PBS irradiated at 10 J/cm^2, Control PBS with PDZ, Control PBS with PDZ illuminated at 10 J/cm^2, Control MRSA, Control MRSA illuminated only, Control MRSA only PDZ 0.25 µg.mL^{-1} and aPDT 0.25 µg.mL^{-1} with a light doseof 10 J/cm^2. (C) Bacterial count after aPDT, showing the PBS Control, MRSA Control, PDZ 0.25 µg.mL^{-1} only, L 10 J/cm^2, and aPDT 0.25 µg.mL^{-1} only with the flow of 10 J/cm^2.

6.7 $\log_{10}$ was observed, which, in addition to viability, also affected the bacterial metabolic capacity as assessed by the resazurin reagent. Bacterial metabolism is directly related to bacterial virulence factors' production capacity, especially biofilm formation.

Metabolic assessments performed with resazurin, a blue reagent that is irreversibly reduced to highly fluorescent pink resorufin when metabolized by bacterial cells [26], are used to assess the antibiotic susceptibility of microorganisms [27–30]. However, this test has been applied to evaluate bacterial metabolism after aPDT because it is easy to perform, and biofilms can be tested *in situ* by removing them from surfaces, allowing assessment of total metabolism and avoiding problems associated with variations in biofilm removal [31]. In this sense, Magacho et al. evaluated the bacterial metabolism after aPDT with methylene blue (MB) in Gram-negative bacteria [23]. They concluded that it is possible to observe a reduction in bacterial metabolism after applying the therapy. Moreover, Nie et al. [31] applied aPDT mediated by Ce6 (50 mM) combined with H_2O_2 (0.3–33.3 mM) with a light doseof 15 J/cm2 (450 nm or 660 nm) to multi-species biofilms. As a result, the combination of 33.3 mM H_2O_2 and Ce6-aPDT had more significant antimicrobial activity than the isolated compounds, which was appreciated by the reduction of the metabolic capacity evaluated by the resazurin method.

On the other hand, Souza et al., evaluated bacterial metabolism with resazurin after aPDT and bacterial viability with CFU/mL, which demonstrated complete inactivation in the planktonic culture of *S. aureus* with PDZ [15].

Thus, the decrease in bacterial viability is directly related to the decrease in metabolism. However, the reduction in metabolic capacity does not always indicate a reduction in total inactivation. However, the present study demonstrated a decrease in biofilm metabolism with a significant difference of approximately 420 a.u. concerning the non-irradiated control, also corroborating the CFU/mL results. Based on the results, the current antimicrobial photodynamic treatment caused a decrease in bacterial metabolism, viability, replication, and slight disruption (by SEM) of the biofilm structure, which contributed to the inactivation of the mature biofilm.

Although the current study showed a slight biomass reduction by SEM visualization, it was impossible to observe the same reduction by CV test. This can be explained by mature biofilms comprising extracellular matrix, viable and dead cells [32,33]. In this way, bacteria with impaired viability or dead cells may remain attached to the biomass and be stained by CV. This could justify the divergence with SEM images where the biofilm structure could be disrupted in the sample preparation. In this study, the biomass results obtained using the CV method are consistent with the report of Quishida et al., evaluated the response of one and three applications of aPDT with PDZ (175 and 200 mg.mL^{-1}) and irradiation of 37.5 J/cm^2 (660 nm) in multispecies biofilms of *S. mutans*, *C. albicans*, and *C. glabrata*. The authors observed that applying aPDT did not significantly reduce biomass, as in the present study. However, there were significant differences in the three applications compared to the control group, suggesting that serial applications of aPDT can promote biomass reduction and total bacterial inactivation [34].

4.2. ROS Production During aPDT

It is known that the production of ROS is essential for the efficacy of aPDT and that *S. aureus* strains have defense mechanisms, such as the production of a carotenoid pigment called staphyloxanthin. This secondary metabolite is essential in evading the immune system and contributes to bacterial survival [7]. This pigment is a virulence factor that reduces singlet oxygen penetration and decreases membrane fluidity. In addition, the carotenoid can chelate singlet oxygen in the excited state, returning it to the ground state and dissipating energy as heat [35]. Therefore, this compound may significantly reduce the cytotoxicity caused by the therapy, affecting its efficacy against *S. aureus* strains. Therefore, studies are needed to assess the presence of pigment in each strain.

Concomitantly with the action of staphyloxanthin, other enzymatic mechanisms may promote the reduction of ROS. Recently, Rapacka-Zdonczyk et al. reported that sessile bacteria in the biofilm increased the expression of superoxide dismutase (SOD) and catalase enzymes, which catalyze $O^{2\bullet}$, $HO^{\bullet}$, and H_2O_2 to H_2O and molecular oxygen, favoring bacterial survival by eliminating the ROS generated by PS [36]. This fact would explain the increase in survival in the biofilm compared with the planktonic form despite adequate interaction of PS. In this sense, Miñan et al., in 2015, carried out a quantitative analysis of the consumption of $O^{2\bullet-}$ in the *S. aureus* biofilm environment, noting that both the components of the culture medium and the EPS of the biofilm decreased the concentration of $O^{2\bullet-}$ by approximately 50% and 35%, respectively, compared to the concentrations found in PBS. Therefore, it can be speculated that the combination of the described mechanisms favors the survival of the bacteria in the biofilm [37].

In a recent study, no significant difference in ROS production was observed when comparing PDZ concentrations (25, 50, and 100 µg.mL^{-1}) [15]. However, a difference in production was observed when the

fluency used was changed. For all PDZ concentrations, there was a significant increase in ROS at 100 J/cm^2 compared to other lower light doses, reaching complete bacterial inactivation. A similar result was observed by Freitas et al.[38] when they analyzed ROS formation after applying aPDT with curcumin at a higher light dose. Finally, in the current study, PDZ at a concentration of 75 μg.mL^{-1} proved to be an excellent PS for generating ROS when irradiated at 100 J/cm^2; comparing the number of viable sessile cells, the amount of ROS generated reduced bacterial viability by 6.54 log10. Based on the dependent light dose factor, it is suggested that higher light doses may increase ROS production to reach the level necessary for biofilm inactivation.

4.3. Sessile Bacteria Density in Mature Biofilm for aPDT

An important factor to consider when evaluating aPDT is the number of sessile bacteria in the mature biofilm. Souza et al. applied aPDT to *S. aureus* strains (ATCC 25923) with PDZ and showed better performance when irradiated with red LED (660 nm) and light doses (25, 50, 75, and 100 J/cm^2) [13]. Although Bokan et al. mention that the absorption spectra of IQCy, Ce6, and HITC overlap with the emission spectrum of the LED used for excitation, the PS absorption peak used by Souza et al. proved to be more effective as it achieved complete bacterial inactivation [39]. In the current study, irradiation was applied at the maximum absorption peak for the PS Ce6, using a higher experimental inoculums presenting 10^{11} bacteria/well in biofilm after 48 h, achieving a more significant bacterial reduction for the clinical strain of *S. aureus*, compared to Bokan's study, which used the inoculum of 10^4 to 10^5 CFU/mL. It demonstrates the importance of using the appropriate wavelength in the PS absorption spectrum to achieve the correct absorption of the photosensitizer.

Developing an effective aPDT against bacterial infections, especially those associated with biofilms, primarily requires *in vitro* evaluation of photosensitizers and radiation light dose sufficient to eradicate planktonic bacteria and early and mature biofilms. It has also been established that an infection is clinically relevant when the number of bacteria at the site of infection is $\geq 10^5$ CFU [40,41]. Therefore, in our work, we have established a mature biofilm composed of sessile bacteria that significantly exceeds this limit to simulate a situation of high surgical risk, closer to those found in implant infections (*e.g.*, prostheses) or in industrial equipment (*e.g.*, pipeline corrosion). Thus, the photodynamic action of PDZ was evaluated in a very challenging condition, using a mature *S. aureus* biofilm with a high bacterial load and abundant presence of EPS, obtaining an excellent reduction in biofilm viability of approximately 6 log.[10]

4.4. Differences and Challenges Between in vitro and in vivo Models for aPDT Implementation

It is important to note that the morphology, size (extent), and thickness of our *in vitro* biofilm model far exceed those of *in vivo* bacterial infections. In the case of a static *in vitro* model, the biofilm is three-dimensional with a classic mushroom structure, its extension is of the order of 1 cm^{2,} and its thickness is up to 300 μm. In contrast, in an *in vivo* model, numerous bacterial aggregates with an average length between 5 and 50 μm are observed without a typical mushroom structure [42]. Morphological differences in the biofilm would be explained by the presence of the host immune system and limitations on nutrient availability under *in vivo* conditions [43]. Given the above, using *in vitro* models of biofilms to assess antimicrobial treatments on abiotic surfaces colonized by microorganisms is more appropriate. This is particularly relevant in the industrial sector, where the growth and spread of microorganisms are only limited by nutrient access and influenced by the efficacy of anti-biofilm treatments commonly applied. On the other hand, when implementing an aPDT in the health area, it will be necessary to adjust the concentration of photosensitizers and irradiation, considering the characteristics above of the *in vivo* biofilm and in addition to the advantage of having an immune system capable of controlling the infection, once the aPDT is completed. For this reason, a second step before clinical implementation would be to evaluate aPDT using an *in vivo* model that would allow us to adjust the treatment conditions to eradicate bacterial infection.

4.5. aPDT Applied to the MRSA Inactivation in the in vivo G. mellonella Mod

In the second phase of our work, we evaluated the efficacy of aPDT with PDZ on *G. mellonella* larvae infected with an MRSA strain. This invertebrate model of *G. mellonella* is increasingly being used for *in vivo* research because it has an effective immune system consisting of hemocytes, which, in this case, allows us to understand the effects of the therapy [44,45]. Despite the action of the immune system of *G. mellonella*, the pathogens can manage to install the infection and lead the insect to death. Some of the possible causes of the failure of the immune system include difficulty in recognition by the immune system due to changes in the cell walls of the pathogenic agents, the action of multiple virulence factors, high exposure to microbes, the presence of multiple species, *etc.*[45,46].

First, in the current study, the susceptibility of *G. mellonella* to infection by MRSA strains was evaluated at concentrations of 10^4, 10^5 and 10^6 cells/larvae. It was observed that the survival rate of the larvae depended on the amount of MRSA applied. At the concentration of 10^4, the period of total larval lethality was 120 h after inoculation. In comparison, at 10^5 bacterial cells, the period was 96 h, and at 10^6 bacterial cells, it was the most pathogenic concentration for the larvae with lethality in 48 h. From these data, the 10^5 cells/larvae concentration was selected for all subsequent assays since a concentration of intermediate pathogenicity is of interest for evaluating the effect of aPDT. For example, suppose the concentration of the pathogen is low pathogenic. In that case, it may not cause any damage to the host, but if it is highly pathogenic, it may cause mortality before the therapy application. Dos Santos, in 2017, evaluated the aPDT with MB in a model of *G. mellonella* after infection with *P. gingivalis* and described the importance of standardizing the infection in this animal model to avoid the death of the specimens before the therapy can be applied. It was observed that an inoculum of 10^2 bacterial cells did not cause infection in the host, while 10^6 bacterial cells caused complete lethality. Thus, the authors selected a concentration of 10^4 for inoculation since it exhibited intermediate pathogenicity [46]. Therefore, it is fundamental to determine the bacterial concentration to be inoculated since the pathogenicity varies for each species and strain depending on the resistance and virulence factors present.

In the current study, different concentrations of PDZ and light dosesthat did not demonstrate toxicity to the larvae when in the absence of the microorganism were evaluated. Thus, the parameters initially used for applying aPDT were selected according to the *in vitro* method, with PDZ concentrations of 50 and 75 μg.mL^{-1} and light doses of 50 and 25 J/cm^2. Despite the reduction in the MRSA biofilm, the aPDT groups were toxic to *G. mellonella* larvae, with total lethality within 24 h. However, after the successive reduction of the parameters, a beneficial action of the therapy was achieved with parameters 5, 0.25, 2.5 × 10^{-7} μg.mL^{-1} at a light dosesof 10 J/cm^2, highlighting the concentration of 0.25 μg.mL^{-1}, which ensured the survival of 40% of the larvae in the period of up to 168 h, demonstrating the potential of therapy with PDZ for the treatment of MRSA infections.

Garcez et al. 2020 evaluated the effect of aPDT with MB (100 μM) in combination with antibiotics in *G. mellonella* larvae infected with multidrug-resistant strains of *E. coli* [47]. The irradiation parameters were 3 and 18 J/cm^2 and 100 mW/cm^2 (660 nm). As a result, they observed that groups receiving antibiotics or aPDT alone did not improve larval survival, but the combined therapy significantly increased the survival curve. In addition, in *in vitro* tests with *E. coli*

biofilm, they observed by electron cryo-tomography that fluorescent images show that aPDT seems to promote micro-damage to the cell envelope and causes the production of membrane vesicles that permeabilize cell membranes, demonstrating the ability of aPDT to damage the bacterial structure. Chibebe et al. 2013 used *G. mellonella* to evaluate the action of aPDT with MB in infections by multidrug-resistant strains of *Enterococcus faecium*, also evaluating the effect in combination with antibiotics [48]. They conclude that aPDT prolonged larval survival and, when associated with antibiotic treatment, showed that in a vancomycin-resistant strain, aPDT combined with the same drug made the bacteria more susceptible to the antibiotic. Therefore, it is suggested that pretreatment with aPDT may alter the pattern of bacterial resistance to antibiotics, and it is interesting to conduct studies with MRSA strains.

4.6. The Immune System of G. mellonella

The immune system of *G. mellonella* is divided into a cellular immune response and a humoral immune response. The cellular immune response is mediated by phagocytic cells, the hemocytes, responsible for engulfing invaders and assisting in encapsulation and coagulation [49–51]. Phagocytosis by hemocytes occurs similarly to the mammalian immune system, with engulfment and degradation of the invader. This degradation can occur by the action of enzymes or by the generation of ROS. Hemocytes can produce p47 and p67 proteins, which promote the production of superoxide (NADPH oxidase), generating an oxidation reaction and forming ROS-like neutrophils in mammals. In encapsulation, the initial action of the hemocytes can trigger the release of cytotoxic materials by the defense mechanism of microorganisms, such as polysaccharides, peptides, and proteins [10,12,50].

In this work, hemocyte analysis showed a significant increase (2-fold, 8.6×10^7) in hemocytes after aPDT application compared to the CTRL MRSA group (4.1×10^7), suggesting that the application of the therapy stimulated the increase in the immune response, helping to fight the infection.

In this sense, Alvarenga applied aPDT with MB in *G.mellonella* infected by *P. gingivalis* [46]. After performing the aPDT, a 25% increase in larval survival was observed in the control group. However, despite the effect on survival, the hemocyte analysis after aPDT did not show an increase in the immune response. The control group obtained 3.0×10^4 hemocytes, while the aPDT group obtained 1.9×10^4 hemocytes. Thus, although an increase in the immune response with the aPDT was observed in the current study, the application of therapy may not affect the increase in the hemocytes, suggesting that the choice of the PS and the parameters used are critical for the performance of aPDT.

During infection, the cellular and humoral immune responses are mutually regulated, with hemocytes synthesizing and secreting humoral molecules such as proteins, antimicrobial peptides (AMPs), and melanin into the hemolymph. AMPs have the function of disrupting pathogenic membranes and are selectively toxic, affecting only the cells of the microorganism. Its action is faster than the doubling time of the microorganism, and there are no reports of bacterial resistance to AMPs. A large portion of this molecule is produced in the fat body and destined for the hemolymph [45,52]. The melanization process is also part of the humoral immune system and is carried out by a cascade, regulated by the enzyme phenoloxidase (PO), in which, after infection or injury to the area, there is a coagulation process, formation of capsules, phagocytosis or lesions, melanization occurs. Thus, melanization is an essential indicator of infection or injury and can be visually identified [11,53].

The health scale used in the *in vivo* assays was based on the study by Loh et al. (2013), which proposed an analysis of the health of larvae based on their appearance [17]. The characteristics observed were the movement of the animal, ability to form cocoons, presence of melanization, and survival, with scores ranging from 0 to 10. In addition, it was observed that larvae treated with PBS alone maintained their overall health with scores of approximately 10 over the seven days observed. The other groups showed a pattern of decreasing health over the days, except for the PDT group (0.25), which obtained an initial score of approximately 7. They maintained a score of 4 over the seven days, demonstrating that aPDT with chlorin has the potential for clinical application.

The enumeration of MRSA cells in the hemolymph test was performed to observe the presence of bacteria after therapy application. The groups subjected to MRSA infection maintained around 6 $\log_{10}$, regardless of the application of light or PDZ alone. When exposed to aPDT, a slight bacterial reduction was observed, but not significant compared to the MRSA Control. However, compared to the survival results of *G.mellonella*, it was observed that in the long term, one therapy application was beneficial, extending the survival beyond 120 h.

This behavior can be explained by effects associated with aPDT, such as: i) the decrease in the growth rate of surviving bacteria because of radiation [54,55]; ii) a possible progressive decrease in bacterial viability after aPDT. Tosato et al.observed that applying aPDT to mature *Klebsiella pneumoniae* biofilm had a bactericidal effect immediately after the end of the treatment and a biofilm-eradicating action after 24 h [56]. Therefore, the individual or combined action of these factors affecting bacterial growth would allow the immune system to contain and eradicate the infection, which was not observed in the control group with MRSA; and iii) it was also observed in murine models, high survival of mice, even if aPDT did not cause the complete eradication of the microorganisms causing the infection [57,58], indicating a crucial role of the immune system in the resolution of the infectious process.

In this sense, a significant increase in hemocytes is observed when comparing the results of hemocyte analysis and MRSA cells in the hemolymph. Both were evaluated 30 min after the application of aPDT. No significant reduction in bacteria (CFU/mL) was observed. The difference in the results of these experiments is probably due to the increase in the immune system of the larvae as a result of the therapy stimulus. However, 30 min may not have been long enough for the hemocytes to act and contribute to bacterial inactivation, justifying that the late action of hemocytes could prolong larval survival. Chibebe et al. 2013 applied aPDT in models of *G. mellonella* infected with *E. faecium* and evaluated CFU/mL of hemolymph at different hours (0, 2, 4, 8, 12, 24 h) after application of the therapy. The 2 h period showed the lowest CFU/mL, while the 8 h period showed the highest CFU/mL. Therefore, evaluating the CFU/mL of hemolymph at different times would be interesting. In addition, despite the decrease in CFU/mL at 2 h, there was an increase in infection at 8 h. Thus, the serial application of therapy becomes interesting to avoid the increase in infection.

In 2013, Chibebe Junior et al. evaluated the number of fungal cells recovered from the hemolymph of *G. mellonella* infected with *C. albicans* immediately after applying aPDT. In this case, the aPDT group showed a significant reduction of the microorganism compared to the non-irradiated group [59]. Therefore, evaluating the specific reaction time for each microorganism is interesting. For this reason, new tests are proposed to evaluate the long-term bacterial counts after aPDT and the hemocyte analysis to justify hemocytes' help in inactivation. In addition, the serial application of the therapy would be interesting, aiming not only at the production of ROS for inactivation but also at the serial stimulation of the immune system of the larvae, suggesting the need to establish adequate parameters of light and PS, in addition to the time between treatments aPDT sessions.

Finally, it is important to note that the *G. mellonella* model shows a survival rate similar to the mouse sepsis model when inoculated with 10^8 bacteria. Both models show viability 48 h after infection [60]. Thus, the wide availability of larvae, low cost, and ease of maintenance make the *G. mellonella* model attractive for *in vivo* testing.

5. Conclusion

It was possible to conclude that PDZ, at concentrations of 50 and 75 $\mu g.mL^{-1}$, was not cytotoxic for MRSA biofilms. However, when exposed

to aPDT with irradiation of 25, 50, and 100 J/cm^2, they showed a significant reduction in CFU biofilm viability. A maximum reduction of 6.71 $\log_{10}$ was observed in the irradiation parameters of 100 J/cm^2 and PDZ at 75 μg.mL^{-1}, with a reduction in bacterial metabolism, produces high amounts of ROS, capable of affecting bacterial viability and reducing the biomass evaluated by SEM.

Applying aPDT in the invertebrate model of *G. mellonella* demonstrated that the parameters that proved effective in the *in vitro* biofilm model exhibited toxicity to the larvae. However, after successive reductions of PDZ concentration and light doses, parameters 0.25 μg.mL^{-1} and 10 J/cm^2 maintained survival of 40% of larvae over seven days. Also, they observed increased immune response and improved larval health.

Considering the results of this study, the *in vitro* biofilm model has the potential to replicate conditions observed in industrial biofouling. This makes it a valuable tool in developing approaches for the effective aPDT inactivation of massive and hard-to-treat biofilms. However, *in vitro* parameters are not useful for the *in vivo* model because a bacterial infection is established with a low inoculum compared to mature biofilms. Nevertheless, these *in vitro* parameters could be useful in setting a threshold to decrease the concentration of PS and light dose for the *in vivo* study. Therefore, aPDT parameters should be adapted to whether the biofilm is formed on an abiotic surface or to treat an *in vivo* bacterial infection.

Finally, the effect therapy was effective, reinforcing the potential of antimicrobial photodynamic therapy as an alternative to treating bacterial infections caused by MRSA. Furthermore, it is possible to suggest the serial application of aPDT with PDZ in future studies to achieve complete biofilm inactivation and *in vivo* invertebrate models as a preliminary step for clinical application in humans.

Funding

Fundação de Amparo à Pesquisa do Estado de São Paulo (FAPESP 2016/12211-4), Coordenação de Aperfeiçoamento de Pessoal de Nível Superior - Brasil (CAPES) - Financie Code 001 and Universidade do Vale do Paraíba - UNIVAP. Conselho Nacional de Desenvolvimento Científico e Tecnológico - CNPq: 350140/2022-7.

CRediT authorship contribution statement

Beatriz Müller N. Souza: Writing – original draft, Methodology. **Alejandro Guillermo Miñán:** Writing – review & editing. **Isabelle Ribeiro Brambilla:** Writing – review & editing, Methodology. **Juliana Guerra Pinto:** Writing – review & editing, Supervision, Methodology, Investigation. **Maíra Terra Garcia:** Methodology. **Juliana Campos Junqueira:** Writing – review & editing, Methodology. **Juliana Ferreira-Strixino:** Writing – review & editing, Supervision, Methodology, Funding acquisition.

Declaration of competing interest

The authors whose names are listed immediately below certify that they have NO affiliations with or involvement in any organization or entity with any financial interest (such as honoraria; educational grants; participation in speakers' bureaus; membership, employment, consultancies, stock ownership, or other equity interest; and expert testimony or patent-licensing arrangements), or non-financial interest (such as personal or professional relationships, affiliations, knowledge or beliefs) in the subject matter or materials discussed in this manuscript.

Data availability

Data will be made available on request.

Acknowledgements

FINEP 01.13.0275/00 and CEPOF (2013/07276–1).

Appendix A. Supplementary data

Supplementary data to this article can be found online at https://doi.org/10.1016/j.jphotobiol.2024.112860.

References

[1] R.R. Watkins, M. Holubar, M.Z. David, Antimicrobial resistance in methicillin-resistant Staphylococcus aureus to newer antimicrobial agents, Antimicrob. Agents Chemother. 63 (2019) 1–14, https://doi.org/10.1128/AAC.01216-19.
[2] A. Hamdan-Partida, S. González-García, E. de la Rosa García, J. Bustos-Martínez, Community-acquired methicillin-resistant *Staphylococcus aureus* can persist in the throat, Int. J. Med. Microbiol. 308 (2018) 469–475, https://doi.org/10.1016/j.ijmm.2018.04.002.
[3] CDC, Antibiotic resistance threats in the United States 2019, Cdc. 10 (2019), https://doi.org/10.1186/s13756-020-00872-w.
[4] Antibacterial Agents in Clinical Development: An Analysis of the Antibacterial Clinical Development Pipeline, World Health Organization, Geneva, 2019.
[5] P. Dharmaratne, D.N. Sapugahawatte, B. Wang, C.L. Chan, K.M. Lau, C. Lau, K. P. Fung, D.K. Ng, M. IP, Contemporary approaches and future perspectives of antibacterial photodynamic therapy (aPDT) against methicillin-resistant Staphylococcus aureus (MRSA): a systematic review, Eur. J. Med. Chem. 200 (2020) 112341, https://doi.org/10.1016/j.ejmech.2020.112341.
[6] M. Jia, B. Mai, S. Liu, Z. Li, Q. Liu, P. Wang, Antibacterial effect of S-Porphin sodium photodynamic therapy on Staphylococcus aureus and multiple drug resistance Staphylococcus aureus, Photodiagn. Photodyn. Ther. 28 (2019) 80–87, https://doi.org/10.1016/j.pdpdt.2019.08.031.
[7] N. Kashef, M.R. Hamblin, Can microbial cells develop resistance to oxidative stress in antimicrobial photodynamic inactivation? Drug Resist. Updat. 31 (2017) 31–42, https://doi.org/10.1016/j.drup.2017.07.003.
[8] F. Alves, J.C. Carmello, G.C. Alonso, E.G. de O. Mima, V.S. Bagnato, A.C. Pavarina, A randomized clinical trial evaluating Photodithazine-mediated antimicrobial photodynamic therapy as a treatment for denture stomatitis, Photodiagn. Photodyn. Ther. 32 (2020), https://doi.org/10.1016/j.pdpdt.2020.102041.
[9] M. Terra Garcia, A.H. Correia Pereira, L.M.A. Figueiredo-Godoi, A.O.C. Jorge, J. F. Strixino, J.C. Junqueira, Photodynamic therapy mediated by chlorin-type photosensitizers against Streptococcus mutans biofilms, Photodiagn. Photodyn. Ther. 24 (2018) 256–261, https://doi.org/10.1016/j.pdpdt.2018.08.012.
[10] O.L. Champion, R.W. Titball, S. Bates, Standardization of g. Mellonella larvae to provide reliable and reproducible results in the study of fungal pathogens, J. Fungi. 4 (2018), https://doi.org/10.3390/jof4030108.
[11] J.C. Junqueira, Galleria mellonella as a model host for human pathogens: recent studies and new perspectives, Virulence. 3 (2012) 474–476, https://doi.org/10.4161/viru.22493.
[12] L. Vertyporokh, I. Wojda, Immune response of galleria mellonella after injection with non-lethal and lethal dosages of *Candida albicans*, J. Invertebr. Pathol. 170 (2020) 107327, https://doi.org/10.1016/j.jip.2020.107327.
[13] A.B. Uzdensky, O.Y. Dergacheva, A.A. Zhavoronkova, A.V. Reshetnikov, G. V. Ponomarev, Photodynamic effect of novel chlorin e6 derivatives on a single nerve cell, Life Sci. 74 (2004) 2185–2197, https://doi.org/10.1016/j.lfs.2003.09.053.
[14] L. Pires, S.D.M.G. Bosco, M.S. Baptista, C. Kurachi, Photodynamic therapy in pythium insidiosum - an in vitro study of the correlation of sensitizer localization and cell death, PLoS One 9 (2014) 1–8, https://doi.org/10.1371/journal.pone.0085431.
[15] B.M. Nunes Souza, J.G. Pinto, A.H. Correia Pereira, A.G. Miñán, J. Ferreira-Strixino, Efficiency of antimicrobial photodynamic therapy with photodithazine® on mssa and mrsa strains, Antibiotics. 10 (2021) 1–17, https://doi.org/10.3390/antibiotics10070869.
[16] I. de P. Ribeiro, J.G. Pinto, B.M.N. Souza, A.G. Miñán, J. Ferreira-Strixino, Antimicrobial photodynamic therapy with curcumin on methicillin-resistant *Staphylococcus aureus* biofilm, Photodiagn. Photodyn. Ther. 37 (2022), https://doi.org/10.1016/j.pdpdt.2022.102729.
[17] J.M.S. Loh, N. Adenwalla, S. Wiles, T. Proft, Galleria mellonella larvae as an infection model for group a streptococcus, Virulence. 4 (2013) 419–428, https://doi.org/10.4161/viru.24930.
[18] G. Wijesinghe, A. Dilhari, B. Gayani, N. Kottegoda, L. Samaranayake, M. Weerasekera, Influence of laboratory culture media on in vitro growth, adhesion, and biofilm formation of *Pseudomonas aeruginosa* and *Staphylococcus aureus*, Med. Princ. Pract. 28 (2019) 28–35, https://doi.org/10.1159/000494757.
[19] Suryani Dyah Astuti, Hafidiana, Riries Rulaningtyas, Abdurachman, Alfian P. Putra, Samian, D. Arifianto, The efficacy of photodynamic inactivation with laser diode on *Staphylococcus aureus*biofilm with various ages of biofilm, Infect. Dis. Rep. 12 (2020) 8736, https://doi.org/10.4081/idr.2020.
[20] I. Alav, J.M. Sutton, K.M. Rahman, Role of bacterial efflux pumps in biofilm formation, J. Antimicrob. Chemother. 73 (2018) 2003–2020, https://doi.org/10.1093/jac/dky042.

[21] A.M. Almeida, O.N. Oliveira, P.H.B. Aoki, Role of toluidine blue-O binding mechanism for photooxidation in bioinspired bacterial membranes, Langmuir. 35 (2019) 16745–16751, https://doi.org/10.1021/acs.langmuir.9b03045.
[22] L. Misba, S. Zaidi, A.U. Khan, A comparison of antibacterial and antibiofilm efficacy of phenothiazinium dyes between gram positive and gram negative bacterial biofilm, Photodiagn. Photodyn. Ther. 18 (2017) 24–33, https://doi.org/10.1016/j.pdpdt.2017.01.177.
[23] C. Costa Magacho, J. Guerra Pinto, B. Müller Nunes Souza, A.H. Correia Pereira, J. Ferreira Strixino, Comparison of photodynamic therapy with methylene blue associated with ceftriaxone in gram-negative bacteria; an in vitro study, Photodiagn. Photodyn. Ther. 30 (2020), https://doi.org/10.1016/j.pdpdt.2020.101691.
[24] A.H.C. Pereira, J.G. Pinto, M.A.A. Freitas, L.C. Fontana, C. Pacheco Soares, J. Ferreira-Strixino, Methylene blue internalization and photodynamic action against clinical and ATCC *Pseudomonas aeruginosa* and *Staphyloccocus aureus* strains, Photodiagn. Photodyn. Ther. 22 (2018), https://doi.org/10.1016/j.pdpdt.2018.02.008.
[25] G.Y.C. Cheung, J.S. Bae, M. Otto, Pathogenicity and virulence of *Staphylococcus aureus*, Virulence. 12 (2021) 547–569, https://doi.org/10.1080/21505594.2021.1878688.
[26] R. Csepregi, B. Lemli, S. Kunsági-Máté, L. Szente, T. Koszegi, B. Németi, M. Poór, Complex formation of resorufin and resazurin with b-cyclodextrins: can cyclodextrins interfere with a resazurin cell viability assay? Molecules. 23 (2018) https://doi.org/10.3390/molecules23020382.
[27] J. Germ, L. Poirel, T.C. Kisek, V.C. Spik, K. Seme, M.M. Premru, T.L. Zupanc, P. Nordmann, M. Pirs, Evaluation of resazurin-based rapid test to detect colistin resistance in Acinetobacter baumannii isolates, Eur. J. Clin. Microbiol. Infect. Dis. 38 (2019) 2159–2162, https://doi.org/10.1007/s10096-019-03657-1.
[28] H. Jia, R. Fang, J. Lin, X. Tian, Y. Zhao, L. Chen, J. Cao, T. Zhou, Evaluation of resazurin-based assay for rapid detection of polymyxin-resistant gram-negative bacteria, BMC Microbiol. 20 (2020) 1–11, https://doi.org/10.1186/s12866-019-1692-3.
[29] P. Mishra, D. Singh, K.P. Mishra, G. Kaur, N. Dhull, M. Tomar, V. Gupta, B. Kumar, L. Ganju, Rapid antibiotic susceptibility testing by resazurin using thin film platinum as a bio-electrode, J. Microbiol. Methods 162 (2019) 69–76, https://doi.org/10.1016/j.mimet.2019.05.009.
[30] N.S. Ravi, R.F. Aslam, B. Veeraraghavan, Chapter 6 a new method for detrmination of minimum biofilm eradication concentration for accurate antimicrobial therapy, in: *Acinetobacter Baumannii* Methods Protoc. Methods Mol. Biol, 2019, pp. 61–67, https://doi.org/10.1007/978-1-4939-9118-1.
[31] M. Nie, R.C.e. Silva, K.T. de Oliveira, V.S. Bagnato, A.N. de Souza Rastelli, W. Crielaard, J. Yang, D.M. Deng, Synergetic antimicrobial effect of chlorin e6 and hydrogen peroxide on multi-species biofilms, Biofouling. 37 (2021) 656–665, https://doi.org/10.1080/08927014.2021.1954169.
[32] J.M. Soares, N.M. Inada, V.S. Bagnato, K.C. Blanco, Evolution of surviving Streptoccocus pyogenes from pharyngotonsillitis patients submit to multiple cycles of antimicrobial photodynamic therapy, J. Photochem. Photobiol. B Biol. 210 (2020) 111985, https://doi.org/10.1016/j.jphotobiol.2020.111985.
[33] E. Peeters, H.J. Nelis, T. Coenye, Comparison of multiple methods for quantification of microbial biofilms grown in microtiter plates, J. Microbiol. Methods 72 (2008) 157–165, https://doi.org/10.1016/j.mimet.2007.11.010.
[34] C.C.C. Quishida, E.G. de Oliveira Mima, L.N. Dovigo, J.H. Jorge, V.S. Bagnato, A. C. Pavarina, Photodynamic inactivation of a multispecies biofilm using Photodithazine® and LED light after one and three successive applications, Lasers Med. Sci. 30 (2015) 2303–2312, https://doi.org/10.1007/s10103-015-1811-9.
[35] M. Uenojo, M.R. Maróstica, G.M. Pastore, Carotenóides: propriedades, aplicações e biotransformação para formação de compostos de aroma, Quim Nova 30 (2007) 616–622, https://doi.org/10.1590/S0100-40422007000300022.
[36] A. Rapacka-Zdończyk, A. Woźniak, K. Michalska, M. Pierański, P. Ogonowska, M. Grinholc, J. Nakonieczna, Factors determining the susceptibility of Bacteria to antibacterial photodynamic inactivation, Front. Med. 8 (2021), https://doi.org/10.3389/fmed.2021.642609.
[37] A. Miñán, C. Lorente, A. Ipiña, A.H. Thomas, M.F.L. de Mele, P.L. Schilardi, Photodynamic inactivation induced by carboxypterin: a novel non-toxic bactericidal strategy against planktonic cells and biofilms of Staphylococcus aureus, Biofouling. 31 (2015) 459–468, https://doi.org/10.1080/08927014.2015.1055731.
[38] M.A.A. Freitas, A.H.C. Pereira, J.G. Pinto, A. Casas, J. Ferreira-Strixino, Bacterial viability after antimicrobial photodynamic therapy with curcumin on multiresistant *Staphylococcus aureus*, Future Microbiol. 14 (2019) 739–748, https://doi.org/10.2217/fmb-2019-0042.
[39] M. Bokan, F. Nakonechny, E. Talalai, D. Kobzev, G. Gellerman, L. Patsenker, Photodynamic effect of novel hexa-iodinated quinono-cyanine dye on *Staphylococcus aureus*, Photodiagn. Photodyn. Ther. 31 (2020) 101866, https://doi.org/10.1016/j.pdpdt.2020.101866.
[40] M.C. Robson, C.E. Lea, D. JB, Quantitative bacteriology and delayed wound closure, in: Surgical Forum Vol. 19, 1968, pp. 501–502 (Surg. Forum.).
[41] M.C. Robson, J.P. Heggers, Delayed wound closures based on bacterial counts, J. Surg. Oncol. 2 (1970) 379–383, https://doi.org/10.1002/jso.2930020410.
[42] T. Bjarnsholt, M. Alhede, M. Alhede, S.R. Eickhardt-Sørensen, C. Moser, M. Kühl, P. Ø. Jensen, N. Høiby, The in vivo biofilm, Trends Microbiol. 21 (2013) 466–474, https://doi.org/10.1016/j.tim.2013.06.002.
[43] J.W. Costerton, Z. Lewandowski, D. DeBeer, D. Caldwell, D. Korber, G. James, Biofilms, the customized microniche, J. Bacteriol. 176 (1994) 2137–2142, https://doi.org/10.1128/jb.176.8.2137-2142.1994.
[44] L.M.A. Figueiredo-Godoi, R.T. Menezes, J.S. Carvalho, M.T. Garcia, A.G. Segundo, A.O.C. Jorge, J.C. Junqueira, Exploring the galleria mellonella model to study antifungal photodynamic therapy, Photodiagn. Photodyn. Ther. 27 (2019) 66–73, https://doi.org/10.1016/j.pdpdt.2019.05.010.
[45] K. Kangassalo, T.M. Valtonen, D. Roff, M. Pölkki, I.M. Dubovskiy, J. Sorvari, M. J. Rantala, Intra- and trans-generational effects of larval diet on susceptibility to an entomopathogenic fungus, Beauveria bassiana, in the greater wax moth, galleria mellonella, J. Evol. Biol. 28 (2015) 1453–1464, https://doi.org/10.1111/jeb.12666.
[46] J.D. dos Santos, J.A. de Alvarenga, R.D. Rossoni, M.T. García, R.M. Moraes, A. L. Anbinder, A.O. Cardoso Jorge, J.C. Junqueira, Immunomodulatory effect of photodynamic therapy in galleria mellonella infected with Porphyromonas gingivalis, Microb. Pathog. 110 (2017) 507–511, https://doi.org/10.1016/j.micpath.2017.07.045.
[47] A.S. Garcez, M. Kaplan, G.J. Jensen, F.R. Scheidt, E.M. Oliveira, S.S. Suzuki, Effects of antimicrobial photodynamic therapy on antibiotic-resistant Escherichia coli, Photodiagn. Photodyn. Ther. 32 (2020), https://doi.org/10.1016/j.pdpdt.2020.102029.
[48] J. Chibebe Junior, B.B. Fuchs, C.P. Sabino, J.C. Junqueira, A.O.C. Jorge, M. S. Ribeiro, M.S. Gilmore, L.B. Rice, G.P. Tegos, M.R. Hamblin, E. Mylonakis, Photodynamic and antibiotic therapy impair the pathogenesis of enterococcus faecium in a whole animal insect model, PLoS One 8 (2013), https://doi.org/10.1371/journal.pone.0055926.
[49] J.A. Hoffmann, Innate immunity of insects, Curr. Opin. Immunol. 7 (1995) 4–10.
[50] S. Jemel, J. Guillot, K. Kallel, F. Botterel, E. Dannaoui, Galleria mellonella for the evaluation of antifungal efficacy against medically important fungi, a narrative review, Microorganisms. 8 (2020), https://doi.org/10.3390/microorganisms8030390.
[51] I. Wojda, Immunity of the greater wax moth galleria mellonella, Insect Sci. 24 (2017) 342–357, https://doi.org/10.1111/1744-7917.12325.
[52] P. Singkum, S. Suwanmanee, P. Pumeesat, N. Luplertlop, A powerful in vivo alternative model in scientific research: *Galleria mellonella*, Acta Microbiol. Immunol. Hung. 66 (2019) 31–55, https://doi.org/10.1556/030.66.2019.001.
[53] G. Cotter, S. Doyle, K. Kavanagh, Development of an insect model for the in vivo pathogenicity testing of yeasts, FEMS Immunol. Med. Microbiol. 27 (2000) 163–169, https://doi.org/10.1016/S0928-8244(99)00185-6.
[54] J.T. Pedroso, E. Ponce, I. de P. Ribeiro, J.G. Pinto, A. Guillermo Miñán, J. Ferreira-Strixino, Effectiveness of the blue led in the photoinactivation of Staphylococcus aureus and Staphylococcus epidermidis in vitro, Res. Soc. Dev. 11 (2022), https://doi.org/10.33448/rsd-v11i2.25630 e37511225630.
[55] V.V. Bumah, D.S. Masson-Meyers, S. Cashin, C.S. Enwemeka, Optimization of the antimicrobial effect of blue light on methicillin-resistant *Staphylococcus aureus* (MRSA) in vitro, Lasers Surg. Med. 47 (2015) 266–272, https://doi.org/10.1002/lsm.22327.
[56] M.G. Tosato, P. Schilardi, M.F. Lorenzo de Mele, A.H. Thomas, C. Lorente, A. Miñán, Synergistic effect of carboxypterin and methylene blue applied to antimicrobial photodynamic therapy against mature biofilm of *Klebsiella pneumoniae*, Heliyon. (2020), https://doi.org/10.1016/j.heliyon.2020.e03522.
[57] M.R. Hamblin, T. Zahra, C.H. Contag, A.T. McManus, T. Hasan, Optical monitoring and treatment of potentially lethal wound infections in vivo, J. Infect. Dis. 187 (2003) 1717–1725, https://doi.org/10.1086/375244.
[58] P.S. Zolfaghari, S. Packer, M. Singer, S.P. Nair, J. Bennett, C. Street, M. Wilson, In vivo killing of *Staphylococcus aureus* using a light-activated antimicrobial agent, BMC Microbiol. 9 (2009) 1–8, https://doi.org/10.1186/1471-2180-9-27.
[59] J. Chibebe Junior, C.P. Sabino, X. Tan, J.C. Junqueira, Y. Wang, B.B. Fuchs, A.O. C. Jorge, G.P. Tegos, M.R. Hamblin, E. Mylonakis, Selective photoinactivation of *Candida albicans* in the non-vertebrate host infection model galleria mellonella, BMC Microbiol. 13 (2013), https://doi.org/10.1186/1471-2180-13-217.
[60] J.J. Wanford, R.G. Hames, D. Carreno, Z. Jasiunaite, W.Y. Chung, F. Arena, V. Di Pilato, K. Straatman, K. West, R. Farzand, M. Pizza, L. Martinez-Pomares, P. W. Andrew, E.R. Moxon, A.R. Dennison, G.M. Rossolini, M.R. Oggioni, Interaction of *Klebsiella pneumoniae* with tissue macrophages in a mouse infection model and ex-vivo pig organ perfusions: an exploratory investigation, Lancet Microbe. 2 (2021) e695–e703, https://doi.org/10.1016/S2666-5247(21)00195-6.